

Anomalous photovoltaic effect in ferroelectrics

V. M. Fridkin and B. N. Popov

A. V. Shubnikov Institute of Crystallography, Academy of Sciences of the USSR, Moscow
Usp. Fiz. Nauk **126**, 657-671 (December 1978)

The recently discovered anomalous photovoltaic effect in ferroelectrics is attracting considerable attention of specialists in ferroelectricity and solid-state physics. The anomalous nature of the effect is manifested by the fact that the photo-emf developed in ferroelectrics and pyroelectrics is many orders of magnitude greater than the band gap and can reach 10^3 - 10^5 V. The anomalous photovoltaic effect in ferroelectrics has found extensive applications in volume phase holography. A review is given of the experimental investigations of the anomalous photovoltaic effect in ferroelectrics and also of the models proposed to explain this effect.

PACS numbers: 72.40. + w, 77.80. - e

CONTENTS

1. Introduction	981
2. Short-circuit photovoltaic current	982
3. Anomalous photovoltaic effect in ferroelectrics	985
4. Nature of the anomalous photovoltaic effect in ferroelectrics	987
A. Excitation and recombination at asymmetric impurity centers	987
B. Asymmetry of nonequilibrium electron distribution function	988
C. Photoinduced fluctuations	989
5. Conclusions	990
Literature cited	990

1. INTRODUCTION

Investigations of photoelectric properties of ferroelectrics have recently led to the discovery of the anomalous photovoltaic effect in these materials. This effect is manifested by the appearance of a steady-state current in a homogeneous short-circuited ferroelectric crystal subjected to uniform illumination with wavelengths corresponding to the fundamental or impurity absorption region: in this way a crystal becomes a photo-emf source. If such a crystal is illuminated under open-circuit conditions, an anomalously high photovoltage of 10^3 - 10^5 V is developed, i.e., the photovoltage exceeds by several orders of magnitude the value corresponding to the band gap E_g . The anomalous photovoltaic current and the anomalous photovoltages are observed only in the direction of the spontaneous polarization P_0 of a crystal and disappear in the paraelectric region; the photovoltage is proportional to the length of a crystal in the direction P_0 .

It is clear from this description that the bulk nature of the anomalous photovoltaic effect in homogeneous ferroelectrics differs basically from the corresponding phenomena in semiconductors, such as the Dember photo-emf¹ or the anomalously high photovoltages in films.² The latter are associated either with the illumination nonuniformity or with the inhomogeneity of the crystal itself ($p-n$ junction). For example, anomalously high photovoltages in films are due to the additive effect of elementary Dember emf's or elementary emf's developed across $p-n$ junctions in a texture.²

Uniform illumination of a short-circuited homogeneous ferroelectric produces a steady-state current, which was named photovoltaic in Ref. 3. The photovoltaic current J flows parallel to the spontaneous polarization P_0 and is directly proportional to the illumination intensity I . It is shown in Ref. 4 that this photovoltaic current gives rise to anomalously high photovoltages in a ferroelectric. In fact, in the open-circuit regime a transient photocurrent flows through a ferroelectric in the P_0 direction:⁴

$$J^* = J + (\sigma_d + \sigma_{ph})\bar{E}, \tag{1}$$

where \bar{E} is the macroscopic electric field generated as a result of charging of the capacitance of the crystal by the photovoltaic current J ; σ_d and σ_{ph} are the dark conductivity and photoconductivity, respectively. The photovoltage V which appears in a crystal in this direction during a period equal to the Maxwellian relaxation time ($J^* = 0$) is

$$V = \bar{E}l = \frac{J}{\sigma_d + \sigma_{ph}}l, \tag{2}$$

where l is the distance between the electrodes. According to Eq. (2), V is directly proportional to this distance and is not limited by the band gap.

We shall define the anomalous photovoltaic (AP) effect in ferroelectrics as both the steady-state short-circuit photovoltaic current and the anomalous open-circuit photovoltage (APV) $V \gg E_g$. We must point out that the APV effect in ferroelectrics may, in principle, be related not to the photovoltaic current but to transi-

ent photocurrents of a different origin.^{5,6} In particular, transient photocurrents in a ferroelectric may be observed because of the influence of nonequilibrium carriers (or photoexcited impurity centers) on the spontaneous polarization P_0 . The resultant field $E \approx 4\pi\Delta P_0/\epsilon$ (and the corresponding voltage $V = \bar{E}l$) may give rise to a number of effects, for example, the photorefractive effect.⁵ This photorefractive effect is the change in the optical birefringence of a ferroelectric due to its illumination. Thus, the photorefractive and APV effects may, in principle, be associated with a change in the spontaneous polarization due to illumination and be accompanied by a transient screening current. This mechanism and transient screening currents are indeed observed in ferroelectrics.⁶ However, we shall show later that at least for the majority of the ferroelectrics investigated so far the APV effect is precisely due to the steady-state photovoltaic current. Therefore, in the case of these ferroelectrics an analysis of the mechanism of the AP and, in particular, of the APV effect reduces to an investigation of the nature of the photovoltaic current.

In spite of the considerable amount of experimental material accumulated so far, the nature of the photovoltaic effect in ferroelectrics is far from fully understood and only the first steps have been taken in developing the theory of the AP effect. Therefore, we shall confine our review to a systematic account of the experimental investigations and a comparison with the proposed possible mechanisms on the assumption that this will help the development of the theory of the effect.

2. SHORT-CIRCUIT PHOTOVOLTAIC CURRENT

The photovoltaic current was the name used in Ref. 3 for the steady-state short-circuit current observed in the pyroelectric $\text{LiNbO}_3:\text{Fe}$ and ferroelectric $\text{Ba}_x\text{Sr}_{1-x}\text{Nb}_2\text{O}_6$ (SBN) solid solutions subjected to uniform illumination. A relationship between the photovoltaic and photorefractive effects in LiNbO_3 was suggested in Refs. 7 and 8 but the actual proof of this relationship was given later.⁹⁻¹² Parallel investigations of the steady-state photovoltaic current and APV effect were carried out on lithium niobate¹³ and Eqs. (1) and (2) were used to show that the APV effect was precisely due to the steady-state photovoltaic current; this was explained in Ref. 13 by proposing a new carrier transport mechanism for ferroelectrics. Subsequently, the AP effect (including the photovoltaic current¹) was investigated by many authors.^{4-16,10,11}

Figure 1 shows the results of an investigation⁸ of the kinetics of the photovoltaic current in $\text{LiNbO}_3:\text{Fe}$ when

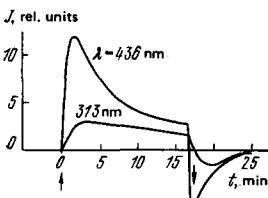


FIG. 1. Kinetics of the photoresponse of LiNbO_3 in the course of measurements of the photovoltaic current.⁸

illumination was started and stopped. Since the Maxwellian relaxation time of $\text{LiNbO}_3:\text{Fe}$ at $T=300^\circ\text{K}$ did not exceed a few minutes ($\sigma \approx 10^{-14} \Omega^{-1} \cdot \text{cm}^{-1}$, $\epsilon \approx 30$), the steady-state photovoltaic current observed in Ref. 8 for tens of minutes could not be the screening photocurrent, as suggested in Ref. 17. Similar results were also obtained in Refs. 7 and 8 for SBN crystals for which the Maxwellian time at $T=300^\circ\text{K}$ did not exceed a few seconds. The kinetics of the transient maximum at the beginning of illumination (Fig. 1) was governed by the relaxation of the photovoltaic current associated with the formation of a space charge in a crystal. Therefore, successive starting and stopping of illumination reduced the transient maximum. This made it possible to vary the transient maximum in estimating the space-charge field \bar{E} . Of course, the pyroelectric current may be superimposed on this transient maximum. Figure 2 shows the spectrum of the steady-state photovoltaic current in $\text{LiNbO}_3:\text{Fe}$ (curve 1), obtained in Ref. 3 and confirmed later in Ref. 4 (curve 2). We shall consider this spectral distribution later. Here, we shall simply note that in the case of $\text{LiNbO}_3:\text{Fe}$ this distribution has a maximum near $\lambda=400 \text{ nm}$, which corresponds to the Fe^{2+} band which is weak or absent from the photoconductivity spectrum (curve 3). However, a correlation has been found^{7,8} between the spectra of the photovoltaic current and the photorefractive effect.

In subsequent investigations^{4,10,11,15,16} the effect was studied by recording the photocurrent-voltage characteristics over a wide range of illumination intensities. Figure 3 shows the photocurrent-voltage characteristics of an $\text{LiNbO}_3:\text{Fe}$ crystal.⁴ In accordance with Eqs. (1) and (2), the photovoltaic current J was deduced from the intercepts on the ordinate and the photovoltage V or field \bar{E} corresponding to the APV effect was deduced from the intercepts on the abscissa. It is clear from Fig. 3 that for illumination intensities I of 1–0.1 W/cm^2 the photovoltaic current varied within the range 10^{-8} – $10^{-9} \text{ A}/\text{cm}^2$, which induced a photovoltage 10^3 – 10^4 V in a crystal $l \approx 1 \text{ cm}$ long. Thus, according to Ref. 4, the lux-ampere characteristic of the photovoltaic current in $\text{LiNbO}_3:\text{Fe}$ is linear and is approximated satisfactorily by the expression

$$J[\text{A}/\text{cm}^2] \approx 10^{-9} I [\text{W}/\text{cm}^2]. \quad (3)$$

In the range of illumination intensities I in Fig. 3 the photovoltage V rises linearly with I . In agreement with

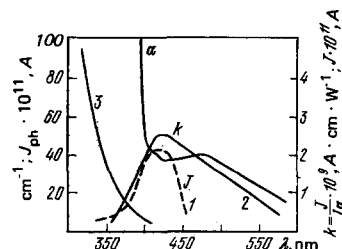


FIG. 2. Spectral distributions of the absorption coefficient α , photocurrent J_{ph} (curve 3), and photovoltaic current J of $\text{LiNbO}_3:\text{Fe}$ (curves 1 and 2). Curve 1 is plotted on the basis of Ref. 3 and curve 2 on the basis of Ref. 4.

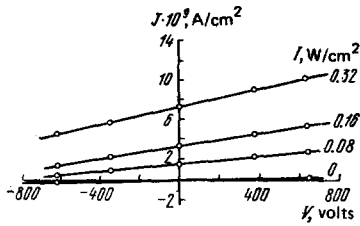


FIG. 3. Current-voltage characteristics of $\text{LiNbO}_3:\text{Fe}$ at $T = 300^\circ\text{K}$ obtained for different intensities of illumination of $\lambda \approx 473 \text{ nm}$ wavelength.⁴

Eq. (2), this corresponds to the low photoconductivity $\sigma_{\text{ph}} < \sigma_d$ of lithium niobate. In the case of $\text{KNbO}_3:\text{Fe}$ the photocarrier lifetime is much higher and, consequently, for $I \approx 1 \text{ W/cm}^2$ we have $\sigma_{\text{ph}} \gg \sigma_d$ and, in agreement with Eq. (2), the dependence $V = V(I)$ shows saturation. This is illustrated in Fig. 4, which is based on Ref. 10. It should be noted that the photovoltage determined by recording the current-voltage characteristics represents the APV effect under open-circuit conditions.

It has been shown¹⁴⁻¹⁶ that the lux-ampere characteristics and temperature dependences of the photovoltaic current J differ considerably from the characteristics of the photocurrent J_{ph} .

Figure 5 shows the lux-ampere characteristics of J and J_{ph} for SBN ($\text{Ba}_{0.25}\text{Sr}_{0.75}\text{Nb}_2\text{O}_6$) crystals in the 4mm tetragonal phase, as well as for SbNbO_4 and BaTiO_3 crystals—all at room temperature. The lux-ampere characteristics of J are in each case linear throughout the investigated range of illumination intensities I , whereas the photocurrent J_{ph} has a sub-linear characteristic $J_{\text{ph}} \propto \sqrt{I}$ (SbNbO_4 , BaTiO_3) or a superlinear region (SBN). Glass *et al.*¹³ obtained the following empirical lux-ampere characteristic for the photovoltaic current in LiNbO_3

$$J = k\alpha I, \quad (4)$$

where α is the absorption coefficient of light, I is its intensity, and k is the Glass constant. For illumination of $\text{LiNbO}_3:\text{Fe}$ in the Fe^{2+} band at $T = 300^\circ\text{K}$ this constant is $k \approx (2-3) \times 10^{-9} \text{ A} \cdot \text{cm} \cdot \text{W}^{-1}$ and is independent of the iron concentration.

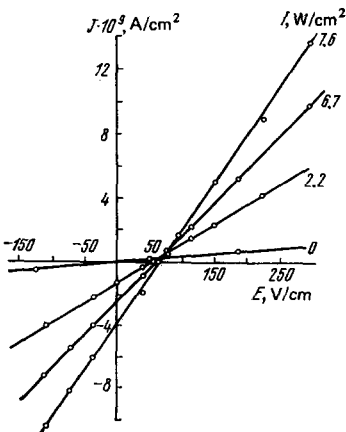


FIG. 4. Current-voltage characteristics of $\text{KNbO}_3:\text{Fe}$ at $T = 300^\circ\text{K}$ obtained for different intensities of illumination of $\lambda \approx 488 \text{ nm}$ wavelength.¹⁰

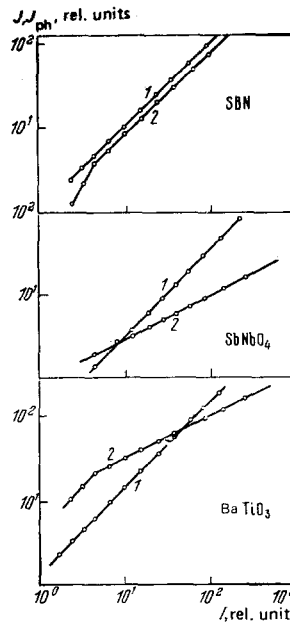


FIG. 5. Lux-ampere characteristics of J (curve 1) and J_{ph} (curve 2) of SBN, SbNbO_4 , and BaTiO_3 (Ref. 14).

Figures 6 and 7 show the temperature dependences of the photovoltaic current J , photoconductivity σ_{ph} , and carrier mobility μ of BaTiO_3 and LiNbO_3 , respectively. The value of σ_{ph} decreases exponentially as a result of cooling, whereas J increases in accordance with a power law when the temperature is lowered. For example, in the case of barium titanate (Fig. 6) the temperature dependence $J = J(T)$ is close to $T^{-3.5}(T - T_1)^{1/2}$, where T_1 is the Curie temperature, in agreement with the temperature dependence of the mobility μ (Ref. 6). Similar results are obtained for SBN, LiNbO_3 , and SbSI when the temperature dependences $J = J(T)$ can be approximated satisfactorily by the T^{-3} law, which is (according to Refs. 6 and 18) close to the temperature dependence of the mobility μ . Figure 7 gives the experimental values of the mobility μ of LiNbO_3 taken from Ref. 19 and these fit well the temperature dependence of the photovoltaic current J obtained in Ref. 16 (the photoconductivity of LiNbO_3 is weak and was not

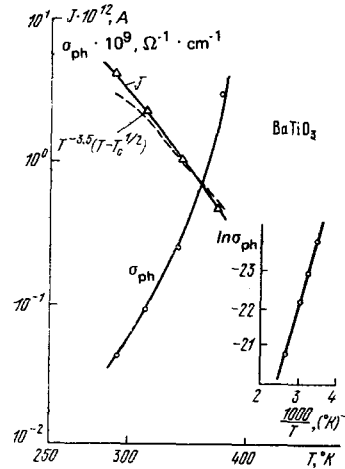


FIG. 6. Temperature dependences of J and σ_{ph} of BaTiO_3 (Ref. 14).

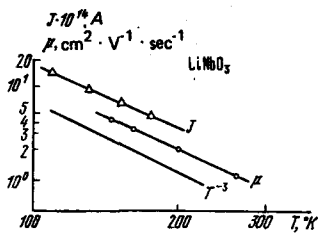


FIG. 7. Temperature dependences of J and μ of LiNbO_3 (Ref. 14).

measured in Ref. 16). It thus follows from the results of Refs. 14–16 that, firstly, the photovoltaic current and photoconductivity vary in opposite ways with temperature and, secondly, the weak—compared with $\sigma_{\text{ph}} = \sigma_{\text{ph}}(T)$ —temperature dependence of $J = J(T)$ may be associated with the temperature dependence of the mobility.

Although the photovoltaic current J depends weakly on temperature, the photovoltage V or the corresponding field \bar{E} should, according to Eq. (2), rise exponentially as a result of cooling. It is shown in Ref. 15 that in the case of SBN and $\text{KNbO}_3:\text{Fe}$ the dependence $\bar{E} = \bar{E}(T)$ is correlated with the temperature dependence of the electrical conductivity during illumination $\sigma = \sigma(T)$ and with the temperature dependence of the photorefractive effect $\Delta n = \Delta n(T)$. This is illustrated in Fig. 8 for SBN. We can see that for SBN all three temperature dependences have the same activation energy $u \approx 0.1$ eV, whereas for $\text{KNbO}_3:\text{Fe}$ this energy is $u \approx 0.06$ eV.

Figure 9 shows the temperature dependence $\bar{E} = \bar{E}(T)$ for SBN in the region of a broad ferroelectric phase transition.¹⁵ In the region of this phase transition the field \bar{E} and the current J have the same temperature dependences due to the phase transition to the paraelectric state in which there is no AP effect (apart possibly from the Demer photo-emf).

There have been quite a few comparative investigations of the photovoltaic current and photoconductivity spectra.^{3,7,10,14,20} Figure 10 shows the spectra of the photovoltaic current J , photocurrent J_{ph} , and field \bar{E} induced in $\text{LiNbO}_3:\text{Fe}$ in oxidized and reduced states.²⁰ As in Ref. 3, the spectrum of J has a maximum at $\lambda \approx 400$ nm, corresponding to the transfer of electrons from the Fe^{2+} levels to the conduction band; this maximum does not appear in the spectrum of J_{ph} .

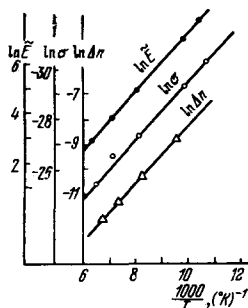


FIG. 8. Temperature dependences of $\ln \bar{E}$, $\ln \sigma$, and $\ln \Delta n$ for SBN (Ref. 15).

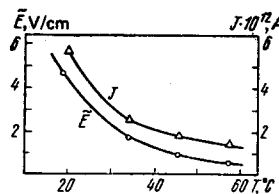


FIG. 9. Temperature dependences of \bar{E} and J near the phase transition of SBN (Ref. 15).

Investigations of the ESR spectra¹⁰ and of the Mössbauer effect²¹ in $\text{LiNbO}_3:\text{Fe}$ has revealed the presence of Fe^{2+} –oxygen vacancy complexes oriented along the [001] direction, with Fe^{2+} replacing Nb^{5+} . A calculation of the energy of such centers²² gives 3.2 eV, which is in agreement with the spectra of J flowing in $\text{LiNbO}_3:\text{Fe}$ (Figs. 2, 9, and 10). There are many data indicating that the Fe^{2+} and Fe^{3+} centers are of donor and acceptor nature, respectively.²³

According to the results in Refs. 19 and 20 (which are in conflict with Ref. 4), J rises beyond the fundamental absorption edge ($\lambda \approx 320$ nm) toward shorter wavelengths although the rise is slower than that of J_{ph} . According to Eq. (2), it follows that the spectrum of the field \bar{E} has a broad maximum. These results indicate a considerable role of the band–band transitions and that the AP effect in lithium niobate can be associated with the impurity and fundamental absorption mechanisms. This is in agreement with the spectra of J and J_{ph} obtained in Ref. 15 for $\text{LiNbO}_3:\text{Fe}$, KNbO_3 , SBN, and SbSI (Fig. 11). For example, the spectra of J and J_{ph} obtained for $\text{KNbO}_3:\text{Fe}$ have an impurity maximum¹⁰ due to complexes formed from Fe^{2+} and oxygen vacancies (at $\lambda \approx 400$ nm), as well as a maximum associated with the fundamental absorption. A comparison of the spectra of J and J_{ph} for the ferroelectric SbSI reveals a considerable difference between the spectra near the fundamental absorption edge ($E_g \approx 2$ eV). The spectrum of J_{ph} has a sharp maximum due to a reduction in the lifetime τ because of surface recombination,⁶ whereas the photovoltaic current rises weakly toward shorter wavelengths. According to Eq. (2), this results in a steep rise of the photovoltage in SbSI in the fundamental absorption region.

In the case of ferroelectric niobates the nature of the

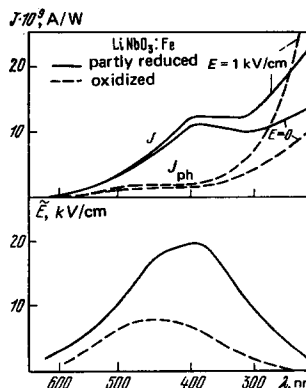


FIG. 10. Spectral distributions of the photovoltaic current ($E=0$), photocurrent in the [001] direction in an external field E , and photoinduced field \bar{E} of $\text{LiNbO}_3:\text{Fe}$ (Ref. 20).

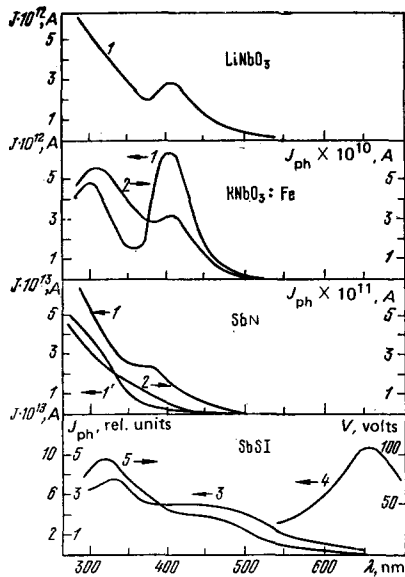


FIG. 11. Spectral distributions of the photovoltaic current J and photocurrent J_{ph} in the [001] direction of LiNbO_3 :Fe, KNbO_3 :Fe (0.1%), SBN, and SbSI : 1) J ; 2) J_{ph} at $T = 300^\circ\text{K}$; 1') J_{ph} at $T = 103^\circ\text{K}$; 3), 5) J and V , respectively, for SbSI at $T = 113^\circ\text{K}$; 4) J_{ph} at $T = 293^\circ\text{K}$ (Ref. 14).

spectrum of J is independent of the polarization of light. The situation is different in the case of BaTiO_3 (Refs. 24 and 25). Figure 12 shows the spectrum of J obtained at $T = 300^\circ\text{K}$ for a BaTiO_3 crystal consisting of a single c -domain in the $\mathbf{E} \parallel \mathbf{c}$ and $\mathbf{E} \perp \mathbf{c}$ cases (the photovoltaic current was measured in the c direction).²⁵ It is clear from Fig. 12 that the photovoltaic current is associated with the fundamental absorption and its maximum corresponds to E_g for BaTiO_3 in the $\mathbf{E} \parallel \mathbf{c}$ and $\mathbf{E} \perp \mathbf{c}$ cases.⁶ However, a change in the polarization of light alters the sign of J . The temperature dependences indicate that the effect appears more strongly at room temperature close to the transition from the tetragonal to the orthorhombic phase. Conversely, a change in the sign of J is hardly noticeable at temperatures close to the transition from the tetragonal to the cubic phase. The photoconductivity of BaTiO_3 is not affected by the polarization of light.

We can thus see that parallel investigations of the photovoltaic current and photoconductivity of an extensive range of ferroelectrics show that they are due to basically different mechanisms. These experiments indicate that the conductivity is governed, as usual,

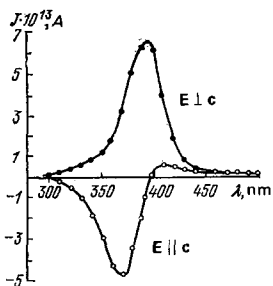


FIG. 12. Spectral distributions of the photovoltaic current of BaTiO_3 for two polarizations of light.²⁵

by the lifetime and mobility of nonequilibrium carriers, whereas the photovoltaic current is independent of the lifetime. In the case of ferroelectrics of the KDP type this difference is particularly strong.²⁶ Such crystals exhibit a considerable photovoltaic current in the ferroelectric phase (and a corresponding anomalous photovoltage $V \approx 10^5$ volts for $l \approx 1$ cm) in the absence of any significant photoconductivity. Conversely, in the paraelectric case when there is no AP effect, the KDP crystals exhibit (at sufficiently high temperatures) a weak photoconductivity.

Apparently the AP effect is common to all the pyroelectric crystals. However, according to Eq. (2), anomalously high photovoltages are observed only when the photoconductivity is sufficiently low. If the photoconductivity is high, the AP effect can be detected only by determining the temperature dependences and the lux-ampere characteristics of the photovoltaic current. This may be why the AP effect has not been observed earlier in such pyroelectric materials as CdS and ZnS in the hexagonal phase. Earlier observations of the photovoltages in ZnS films and crystals^{27,28} have revealed the APV effect associated with the layer structure and additive elementary photo-emf's appearing in the boundaries between the cubic and hexagonal phases. For this reason we shall not consider here the APV effect in ferroelectric ceramics.²⁹

3. ANOMALOUS PHOTOVOLTAGE EFFECT IN FERROELECTRICS

We shall now consider measurements of the photovoltages in ferroelectrics under open-circuit conditions (APV effect).

Photovoltages of $V \gg E_g$ magnitude were first observed³⁰ in an investigation of photoelectric phenomena in single crystals of the ferroelectric solid solution $\text{SbSI}_{0.35}\text{Br}_{0.65}$ and then in BaTiO_3 single crystals.³¹

The sequence of measurements in Refs. 30 and 31 was as follows. An initially polarized single-domain crystal was illuminated in the ferroelectric phase with light corresponding to the photosensitivity maximum. Illumination produced a short-circuit photocurrent along the [001] direction but no special attention was paid in Refs. 30 and 31 as to whether it was steady-state or transient. After the end of illumination the crystal was heated to the paraelectric phase across the Curie point, which was deduced from the pyroelectric current maximum. It was found that illumination shifted the Curie point toward higher temperatures and that this shift ΔT_1 was due to the internal space-charge field \bar{E} . The field \bar{E} was estimated by a method generally used in the case of photoelectrets. A crystal with a shifted Curie point was again illuminated in the paraelectric phase. This produced a depolarization photocurrent which was integrated to find the space-charge density Q_f and, hence, to estimate the internal field $\bar{E} \approx 4\pi Q_f/\epsilon$ and the photovoltage $V = \bar{E}l$. Second illumination of a crystal in the paraelectric phase depolarized the crystal and shifted the Curie temperature back to its equilibrium value. In the case of $\text{SbSI}_{0.35}\text{Br}_{0.65}$ the saturation value of the space charge $Q_f = 1.9 \times 10^{-6}$ C/cm² and the permittivity

$\varepsilon = 2 \times 10^3$ corresponded to a field $\vec{E} \approx 10^4$ V/cm or a photovoltage $V \approx 3 \times 10^3$ volts. The field \vec{E} found in this way and the associated Curie point ΔT_1 determined the coefficient dT_1/dE , in agreement with independent measurements of the Curie point shift under the action of an external field. This indicated that the fields \vec{E} and photovoltages V estimated in Ref. 30 were reliable. Similarly, in the case of BaTiO₃ it was found in Ref. 31 that $E \approx 4 \times 10^3$ V/cm and $V \approx 40$ volts $\gg E_g$, and also that $dT_1/dE \approx +1.2 \times 10^{-3}$ deg \cdot cm \cdot V⁻¹ (Ref. 1), which was close to the rate of shift of the Curie point of BaTiO₃ under the action of an external electric field $dT_1/dE \approx +(1-1.2) \times 10^{-3}$ deg \cdot cm \cdot V⁻¹ (Refs. 1 and 6).

The photovoltage and Curie temperature shift became greater on increase of the illumination intensity. The photovoltage also increased when the intensity of the field used in the preliminary polarization was increased and it reached saturation in fields equal to the saturation polarization and pyroelectric charge. In the cases described above^{30,31} the photovoltage and Curie temperature shift exhibited a slow relaxation in darkness, which was due to localization of nonequilibrium carriers in relatively deep traps.

Subsequently, the APV effect was discovered in lithium niobate,¹³ in several other ferroelectric niobates,³²⁻³⁴ and in the ferroelectric SbSI, and it was also investigated in greater detail in barium titanate.^{24,25,35} Special attention was paid to the relationship between the APV effect and the steady-state photovoltaic current.

Investigations were also made^{32,33} of the kinetics of the APV effect in LiNbO₃:Fe (space group 3 \cdot m), KNbO₃:Fe (2 \cdot m), and antimony orthoniobate SbNbO₄ (2 \cdot m) single crystals.

Illumination was provided by an argon laser at the wavelength 488 nm and the power density was up to 500 mW/cm². The photovoltage was measured in the spontaneous polarization direction [001] and the electrodes were connected to the input capacitance of an electrostatic voltmeter. Some measurements showed that the photo-emf in the orthogonal direction was $V < E_g$. In addition to measurements of the photo-emf of lithium niobate, there were also observations of the photorefractive effect. The same effect in potassium niobate, investigated in Refs. 32 and 33, was measured by Günter *et al.*³⁶ Crystals of SbNbO₄ were optically inhomogeneous so that parallel measurements of the photorefractive effect could not be carried out.³⁴

Figure 13 shows the experimental results obtained for an iron-doped lithium niobate single crystal. Crystals of LiNbO₃:Fe exhibited photovoltages $V \approx 10^3$ volts or higher along the [001] direction (Fig. 13b) when illuminated by a light probe in the form of a spot or a strip parallel to the electrodes and of dimensions $L_1 \approx 1 \times 10^{-2} - 5 \times 10^{-2}$ cm. This probe was focused on the (100) face. Figure 13a shows the kinetics of rise of V during the initial stage of illumination for two intensities (curves 1 and 2). Stopping of illumination at any moment t reduced the photovoltage by an amount corresponding to the pyroelectric charge and then the

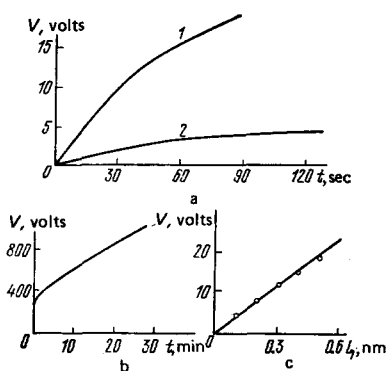


FIG. 13. Anomalous photovoltage (APV) effect in lithium niobate: a) $V = V(t)$ for two illumination intensities $I = 0.15$ and 0.02 W/cm² (curves 1 and 2, respectively); b) $V = V(t)$ after long exposures and high-intensity illumination; c) dependence of $V(\tau_1)$ on L_1 .

value of V relaxed slowly in darkness. Curves 1 and 2 in Fig. 13a give the dependence $V = V(t)$ after subtraction of the pyroelectric signal. The curves in Fig. 13a have two characteristic regions: an initial fast rise followed by a slower rise. A comparison of the kinetics $V = V(t)$ with that of the optical distortion in the same crystal $\Delta n = \Delta n(t)$ (photorefractive effect) shows that the initial fast stage is the same. In the region of the slow rise of $V = V(t)$ the optical distortion has the saturation value $\Delta n = \text{const}$. In the initial fast region the value of $V(t)$ reaches saturation in a relaxation time τ_1 . The value of τ_1 decreases on increase of the illumination intensity. The absolute values of τ_1 were found to be close to the relaxation times of Δn obtained for LiNbO₃:Fe by the compensation method.¹⁷ The values of $V(\tau_1)$ exhibited a linear dependence on the width of the optical probe L_1 (Fig. 13c) and also depended on the illumination intensity I .

Crystals of SbNbO₄ were illuminated with an optical probe in the direction of the spontaneous polarization [001]. The photovoltage V was measured along the same direction. The results of measurements are given in Figs. 14a-14c. We can see that after the beginning of illumination the photovoltage V rises in a time τ_1 to a

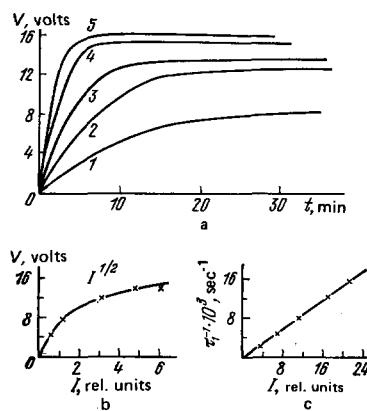


FIG. 14. Anomalous photovoltage (APV) effect in antimony orthoniobate: a) kinetics of APV effect at various illumination intensities $I = 0.02, 0.06, 0.12, 0.2,$ and 0.4 W/cm² (curves 1, 2, 3, 4, and 5, respectively); b) dependence of $V(\tau_1)$ on I ; c) dependence of τ_1 on I .

steady-state value $V(\tau_1)$, which depends on the illumination intensity I (Fig. 14a). After the end of illumination the value of $V(\tau_1)$ relaxes slowly. The pyroelectric effect is slight and does not affect V . Figure 14b gives the dependence of $V(\tau_1)$ on \sqrt{I} , which is close to direct proportionality to I in the range of small values of I , and it is clear from Fig. 14c that the time τ_1 is inversely proportional to I .

In the case of $\text{KNbO}_3:\text{Fe}$ the photovoltage along the [001] direction was several times greater than the band gap. The kinetics of the APV and photorefractive effects in potassium niobate had the same time constant. The photovoltages in BaTiO_3 crystals were found to be^{24,25} of the order of ~10 volts, in agreement with the earlier investigations cited above.³¹ The APV effect in barium titanate depended on the domain structure and was strongest in single-domain high-resistivity crystals.³⁵

According to Eq. (2) the APV effect is inversely proportional to the photoconductivity of all the investigated ferroelectrics and its kinetics is governed by the Maxwellian time constant. A simple relationship links the photorefractive and APV effects in the majority of the ferroelectrics investigated so far. It is found that the illumination-induced change in birefringence is a consequence of the linear electrooptic effect caused by the field \vec{E} , which appears because of the APV effect. This is clear, for example, from Table I where the change in the birefringence Δn is calculated from the linear electrooptic equation for the point symmetry groups given above:

$$\Delta n = \frac{1}{2} (n_1^2 r_{31} - n_3^2 r_{33}) \vec{E}; \quad (5)$$

where n_1 and n_3 are the refractive indices; r_{13} and r_{33} are the electrooptic coefficients; $E = V/l$ is the field induced in the APV effect. It is clear from Table I that the experimental values of Δn for LiNbO_3 and KNbO_3 are in agreement with the calculations.

In all the cases listed above the APV effect is associated with the steady-state photovoltaic current determined for the same crystals in independent experi-

TABLE I. Photorefractive effect Δn and field \vec{E} in APV effect.

Compound	n_1	n_3	r_{13} , mV	r_{33} , mV	ϵ
LiNbO_3	2.29 37	2.22 37	8.6·10 ⁻¹² 37	30.8·10 ⁻¹² 37	30 37
KNbO_3	2.28 38	2.17 38	28·10 ⁻¹² 38	64·10 ⁻¹² 38	100 39
SbNbO_4	—	—	< 2·10 ⁻¹²	< 2·10 ⁻¹²	240 40
Compound	l , cm	$V(\tau_1)$, volts	\vec{E} , V/cm	Δn_{calc}	Δn_{exp}
LiNbO_3	3·10 ⁻²	830	28·10 ⁸	3.3·10 ⁻⁴	10 ⁻³ 17
KNbO_3	5·10 ⁻²	10	200	3·10 ⁻⁶	6·10 ⁻⁶ 36
SbNbO_4	2·10 ⁻²	20	10 ⁸	< 1·10 ⁻⁶	—

ments (see Sec. 2). As pointed out in the Introduction, ferroelectrics may exhibit anomalously high photovoltages associated with other mechanisms (for example, with a change in the spontaneous polarization due to illumination) and not with the steady-state but with the transient screening photocurrent. The question of the relative contributions of other mechanisms to the APV effect in ferroelectrics is outside the scope of the present article.

4. NATURE OF THE ANOMALOUS PHOTOVOLTAIC EFFECT IN FERROELECTRICS

It is pointed out above that the nature of the AP effect is associated with the mechanism of the photovoltaic current in ferroelectrics. Apart from a number of qualitative models, serious investigations have only started.^{41,42} We shall consider some of the models, concentrating on those relevant to the experimental results described above.

A. Excitation and recombination at symmetric impurity centers

A model of the APV effect proposed in Refs. 4 and 13 is based on electron transitions to an allowed band from an impurity center characterized by an asymmetric distribution of the potential. This potential is responsible for asymmetric release of electrons from an impurity level to the band and, consequently, for the steady-state photovoltaic current.

Following Ref. 4, we shall consider the potential of a center in the form of an asymmetric rectangular barrier (Fig. 15). Excitation of an electron between the states ϵ_0 and ϵ_1 (in the $E < V_2$ case) simply shifts a localized electron, as shown by arrows in Fig. 15. This can result in a change in the spontaneous polarization.⁵ If an excited electron has an energy $V_2 < E < V_1$, it is transferred to a free state with a wave vector $+k_1$ (the direction of the wave vector is taken parallel to the spontaneous polarization). An electron with a wave vector $-k_1$ penetrates only partly through the potential barrier. Thus, the probability p_+ of the motion of electrons in the direction $+k_1$ differs from the probability p_- of the motion in the direction $-k_1$ and the difference increases with the spontaneous polarization.

Since the asymmetry of the potential of an impurity center is governed by the direction of the spontaneous polarization and is the same for all the centers, it follows that the density of the photovoltaic current J_1 associated with asymmetric release of electrons by inci-

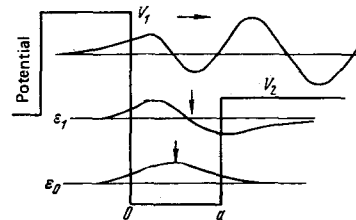


FIG. 15. Asymmetric potential of an impurity center in a ferroelectric and corresponding energies and wave functions.⁴

dent light of intensity I and frequency ω is

$$J_1 = \frac{e\alpha I}{\hbar\omega} (p_+ l_+ - p_- l_-), \quad (6)$$

where l_{\pm} is the mean free path of an electron in the direction $\pm k_1$ and α is the absorption coefficient. We can easily relate J_1 to the spontaneous polarization P_0 . The probabilities p_+ and p_- are associated with the tunnel leakage across rectangular barriers of heights V_1 and V_2 , where $V_2 \ll V_1 \sim P_0^2$, so that

$$J_1 = \frac{e\alpha I}{\hbar\omega} \langle l \rangle P_0, \quad (7)$$

where $\langle l \rangle$ is the average electron displacement.

We must subtract from Eq. (6) the current associated with photocarrier recombination. In fact, after scattering, the directional momentum of a photocarrier is $k_1 = 0$ and prior to recombination it makes no contribution to the photovoltaic current. If we denote the probability of recombination in the directions $+k_1$ and $-k_1$ by p'_+ and p'_- , respectively, we obtain from Eq. (6) the recombination current if we replace p_+ by p'_+ and p_- by p'_- . Finally, we have the following expression⁴ for the photovoltaic current J :

$$J = J_1 - J_2 = k\alpha I, \quad (8)$$

where the Glass constant

$$k = \frac{e}{\hbar\omega} (l_+ p_+ - l_- p_- + l'_+ p'_+ - l'_- p'_-) \quad (9)$$

depends only on the nature of the impurity centers, mean free path, and photon energy.

According to the current-voltage characteristics⁴ of $\text{LiNbO}_3:\text{Fe}$ given in Fig. 3, the Glass constant is $k = 2.5 \times 10^{-9} \text{ A} \cdot \text{cm} \cdot \text{W}^{-1}$ and the total conductivity is $\sigma_d + \sigma_{ph} = 1.3 \times 10^{-14} + 1.2 \times 10^{-12} \Omega^{-1} \cdot \text{cm}^{-1}$. These values are in good agreement with photovoltages calculated for $\text{LiNbO}_3:\text{Fe}$ from Eq. (2). On the basis of the same data the Glass constant k for $\text{LiNbO}_3:\text{Fe}$ is independent of the concentration of the Fe^{2+} donor centers and of the ratio of the Fe^{2+} and Fe^{3+} concentrations. However, this ratio affects strongly the electrical conductivity and photoconductivity of the crystal and, consequently, the APV effect. Chemical reduction of $\text{LiNbO}_3:\text{Fe}$ in a nitrogen atmosphere and an increase in the Fe^{2+} concentration at the expense of Fe^{3+} causes σ_d and σ_{ph} to increase and the values of V and \bar{E} to decrease correspondingly.

Substituting in Eq. (6) the mean free paths $l_{\pm} = (\tau_0 v)_{\pm}$, where $\tau_0 = m\mu/e$ is the relaxation time, v is the electron velocity, and m is the effective mass, we find that

$$J_1 = \frac{e\alpha I}{\hbar\omega} \Delta(p l) = \frac{\alpha m I}{\hbar\omega} \Delta(p v \mu). \quad (10)$$

Under the same conditions the photoconductivity σ_{ph} is of the form

$$\sigma_{ph} = \frac{e\alpha I}{\hbar\omega} \tau \mu, \quad (11)$$

where τ is the lifetime of an electron in a band. It thus follows that the photovoltaic current associated with asymmetric release of an electron is independent of the

lifetime τ , which itself is a function of temperature and illumination intensity. This explains the above difference between the characteristics J and J_{ph} . The lux-ampere characteristic of the photovoltaic current [Eq. (10)] is linear but the corresponding characteristic of the photocurrent [Eq. (11)] is governed by the lifetime $\tau = \tau(I)$, i.e., by the recombination mechanism.¹ The same mechanism determines the temperature dependence of the photocurrent. According to Eq. (10), a weak temperature dependence of the photovoltaic current should be governed by the mobility μ , i.e., by the scattering processes.

The experimental values of k of ferroelectric niobates correspond to an average electron displacement $\langle l \rangle \approx 1 \text{ \AA}$ (Refs. 4 and 10). Therefore, one should mention that in the case of such very small displacements the validity of the band model and of the effective mass approximation is in doubt. Thus, the quantity $\langle l \rangle$ in the Glass model should be associated with the average displacement in the hopping mechanism (small-radius polarons⁴³). The following comment is due here. Equations (8) and (9) are derived assuming implicitly that the quantum yield of electrons is $\gamma = 1$. Ruppel and his colleagues⁴⁴ measured the quantum yield of electrons to the conduction band from the Fe^{2+} centers in LiNbO_3 and found that $\gamma \approx 4 \times 10^{-3}$. According to Eqs. (8) and (9), this corresponds to an average displacement $\langle l \rangle \approx 40 \text{ \AA}$, which is considerably greater than the average jump and, consequently, is in conflict with the Glass model. The nature of the photovoltaic effect is explained in Ref. 44 using the model of photoinduced fluctuations, which we shall discuss later.

B. Asymmetry of nonequilibrium electron distribution function

The photovoltaic current considered in the model of Refs. 4 and 13 is basically of impurity origin because it arises due to the asymmetry of the potential of an impurity center. However, experiments indicate the existence of the photovoltaic current due to absorption in the fundamental region and this current is of the same order as that due to impurity absorption. This difficulty is partly removed in Refs. 41 and 42, where it is shown that not only the asymmetry of the impurity centers responsible for nonequilibrium carrier generation and recombination, but also the asymmetry of the scattering by impurities and phonons, gives rise to the photovoltaic current in ferroelectrics. The asymmetry of the elementary electron processes in ferroelectrics is, in its turn, associated with the asymmetric shape of the potential of the impurity centers and their identical orientation in the lattice relative to the spontaneous polarization direction. This can be demonstrated as follows.^{41,42} The change in the density and distribution of nonequilibrium carriers in the conduction band is described by the kinetic equation for the distribution function $f_{\mathbf{k}}$:

$$\frac{\partial f_{\mathbf{k}}}{\partial t} = I_{\mathbf{k}}^e - I_{\mathbf{k}}^r + I_{\mathbf{k}}^i + I_{\mathbf{k}}^{ph}, \quad (12)$$

where $I_{\mathbf{k}}^e$ and $I_{\mathbf{k}}^r$ are, respectively, the rates of excitation and recombination of electrons; $I_{\mathbf{k}}^i$ and $I_{\mathbf{k}}^{ph}$ are

the numbers of collisions of electrons (per unit time) with impurities and phonons, respectively. If the distribution function is symmetric and satisfies the condition $f_{\mathbf{k}} = f_{-\mathbf{k}}$, no current flows in a crystal. If the right-hand side of the kinetic equation (12) contains an asymmetric term satisfying the condition $I_{\mathbf{k}}^{\text{as}} = -I_{-\mathbf{k}}^{\text{as}}$, the steady-state solutions also have an asymmetric term, which is the asymmetric part of the distribution function $f_{\mathbf{k}}^{\text{as}} = -f_{-\mathbf{k}}^{\text{as}}$. The presence of this asymmetric function gives rise to the steady-state current

$$J = \frac{e}{h} \int \frac{\partial e_{\mathbf{k}}}{\partial \mathbf{k}} f_{\mathbf{k}}^{\text{as}} d\mathbf{k}. \quad (13)$$

It is shown in Refs. 41 and 42 that not only excitation and recombination but also scattering by a dipole center with an asymmetric potential are asymmetric processes and, consequently, give rise to an asymmetric component of the distribution function, i.e., they produce a steady-state current. It is essential to note that we are speaking all the time of the nonequilibrium distribution function. It is demonstrated rigorously in Ref. 44 that in the case of equilibrium electrons we have $f_{\mathbf{k}}^{\text{as}} = 0$, and, consequently, the equilibrium (dark) current is zero. This corresponds to the equilibrium case of Eq. (8) when the current associated with the excitation of electrons from asymmetric centers is compensated exactly by the current due to electron recombination. The theory developed in Refs. 41 and 42 therefore predicts the impurity and intrinsic (due to fundamental absorption) photovoltaic currents. However, in the latter case (band-band transitions) the photovoltaic current is proportional to the square of the relaxation time $J \propto \tau_0^2$. Thus, according to Refs. 41 and 42, the photovoltaic current resulting from the fundamental absorption should be several orders of magnitude lower than that due to the impurity effect, but this is in conflict with the experimental results.

In spite of the fact that the experimental data^{15,20,26,45} indicate the existence of an intrinsic photovoltaic current of the same order of magnitude as the impurity current, they require further refinement. For example, it is worth noting an increase in the photoconductivity and photovoltaic current in the ultraviolet part of the spectrum, corresponding to strong surface absorption (see Fig. 11). This effect is manifested by all the investigated oxygen-octahedral ferroelectrics and its origin is not clear.

The results of Refs. 41 and 42 are generalized in Refs. 46 and 50 to nonpyroelectric crystals without an inversion center. Expanding the current J in powers of the external field

$$J = \sigma_{ik} E_k + \alpha_{ijk} E_j E_k, \quad (14)$$

we can show that the third-rank tensor components α_{ijk} generally differ from zero for crystals belonging to one of the 21 acentric point symmetry groups. If the external field is static, Eq. (14) represents a quadratic correction to Ohm's law. If E_k is understood to be the component of the field of an optical wave, it follows from Eq. (14) that homogeneous illumination of a homogeneous piezoelectric crystal (which need not be pyroelectric) produces the photovoltaic current J

(this current J is called photogalvanic in Refs. 42 and 46). As in Refs. 41 and 42, the microscopic mechanism of the photovoltaic current is attributed to the asymmetry of the excitation and recombination of nonequilibrium carriers at impurity centers. The photovoltaic current flows in the direction in which the component of the tensor of the effective octupole moment of an impurity center \bar{Q}_{ijk} differs from zero,

$$\bar{Q}_{ijk} = \frac{1}{e^2} \left[d_i d_j d_k + \frac{e}{6} (D_{ij} d_k + D_{ik} d_j + D_{kj} d_i) + \frac{e^2}{10} Q_{ijk} \right], \quad (15)$$

where d_i , D_{ij} , and Q_{ijk} are, respectively, the dipole, quadrupole, and octupole moments of the impurity center. The AP effect has been observed experimentally in nonpyroelectric crystals.⁵¹

C. Photoinduced fluctuations

We shall conclude our discussion by considering the model of photoinduced fluctuations.^{24,25,27} We shall turn back to Fig. 15. We shall assume that the absorption of light transfers an impurity-center electron from the ground to an excited state. The corresponding change in the dipole moment of the center by an amount $\Delta\mu_0$ results⁵ in the formation of a localized region of volume V_0 where the spontaneous polarization changes by an amount $\Delta P_0 = \Delta\mu_0/V_0$ and where a field $\bar{E} \approx 4\pi\Delta P_0/\epsilon$ is generated (this is known as a photoinduced fluctuation). If the sign of ΔP_0 (which is the same for all the impurity centers because of symmetry considerations) corresponds to a shift of the energy band edge toward the excitation level, the excited electron is found in the band where it is displaced by the field \bar{E} within the fluctuation limits. Another possible conduction mechanism is the polaron effect, when photoexcitation induces both a fluctuation and a transition of an excited electron to a polaron energy band.⁴³

Irrespective of the conduction mechanism, the expression for the steady-state photovoltaic current J is

$$J = \frac{\Delta P_0}{e} e\mu N_{st}^*, \quad (16)$$

and the kinetics of formation of fluctuations is described by the equation

$$\frac{dN^*}{dt} = \frac{SI}{h\omega} (M - N^*) - \frac{N^*}{\tau_e}, \quad (17)$$

where N^* is the concentration of photoinduced fluctuations; N_{st}^* is its steady-state value; μ is the carrier mobility; M is the concentration of impurity centers; τ_e is the lifetime of a fluctuation equal to the lifetime of an electron in an excited state; I is the illumination intensity; S is the cross section of the interaction of an impurity center with a photon. The steady-state concentration of fluctuations is given by

$$N_{st}^* = \frac{SI/h\omega}{(SI/h\omega) + (1/\tau_e)} M. \quad (18)$$

Substitution of N_{st}^* in Eq. (16) gives the expression for the photovoltaic current. We can easily see that for $1/\tau_e \approx 10^4 - 10^9 \text{ sec}^{-1}$ (Ref. 48), $S \approx 10^{-15} \text{ cm}^2$, and $I \lesssim 1 \text{ W/cm}^2$, the photovoltaic current is a linear function of I :

$$J \approx \frac{\Delta\mu_0}{V_0 e} e\mu \frac{SI}{h\omega} \tau_e M. \quad (19)$$

Let us now substitute in Eq. (19) the following constants for $\text{LiNbO}_3:\text{Cu}^{3+}$: $\Delta\mu_0 \approx 10^{-27} \text{ C}\cdot\text{cm}$, $M \approx 8 \times 10^{19} \text{ cm}^{-3}$,

$\tau_e \approx 10^{-5}$ sec (Ref. 48), $S \approx 10^{-14}$ cm², $\epsilon \approx 30$, and $\hbar\omega \approx 5 \times 10^{-12}$ erg. Then, Eq. (19) reduces to the form

$$J_{[A/cm^2]} \approx \frac{\mu}{V_0} I [W/cm^2]. \quad (20)$$

Let us compare Eq. (20) with the experimental lux-ampere characteristic of the photovoltaic current in LiNbO₃:Fe given by Eq. (3). We can do this by substituting in Eq. (20) the mobility in LiNbO₃ for which contradictory values are given in the literature. For example, substituting $\mu \approx 10^{-3}$ cm²·V⁻¹·sec⁻¹ (Ref. 44), we find that Eqs. (20) and (3) agree for $V_0 \approx 10^{-24}$ cm³, which corresponds to an average fluctuation radius $\langle l \rangle \approx 1$ Å. Thus, in this case $\langle l \rangle$ is close to the average displacement of an electron predicted by the model of an asymmetric center and the fluctuation model gives no new information. However, if we use $\mu \approx 0.8$ cm²·V⁻¹·sec⁻¹ (Ref. 19), the agreement between Eqs. (20) and (3) is obtained for $V_0 \approx 10^{-21}$ cm³ and $\langle l \rangle \approx 10$ Å. Finally, if we follow Ref. 49 and assume $\mu \approx 15$ cm²·V⁻¹·sec⁻¹, then $V_0 \approx 10^{-20}$ cm³ and $\langle l \rangle \approx 10$ – 100 Å, which is in agreement with the postulated dimensions of photoinduced fluctuations in BaTiO₃ (Refs. 24, 25, and 44). It is important to note that in this case the photovoltaic current is due to the motion of carriers under the action of a finite macroscopic field, which distinguishes the fluctuation model from the model of an asymmetric impurity center. It is possible that the scatter of the values of μ for LiNbO₃ is associated with different concentrations of impurity centers and other defects, and with different conditions for the chemical reduction of crystals in a hydrogen atmosphere. Moreover, one should bear in mind that in comparing Eq. (20) with Eq. (3) we are using parameters corresponding to the excitation of the Cu²⁺ ions in LiNbO₃, and also utilizing the mobility in LiNbO₃:Fe.

5. CONCLUSIONS

We can summarize the work on the AP effect (which is mainly experimental) by listing the main results about which there is no controversy.

It has been established reliably that a steady-state photovoltaic current is generated by uniform illumination of a homogeneous ferroelectric in the absence of an external field. It has been shown that the anomalous photovoltages in ferroelectrics, which are several orders of magnitude greater than the band gap, are associated with the charging of a crystal by the photovoltaic current. The mechanisms of the photovoltaic current and photocurrent in a ferroelectric are basically different, and the explanation of the former requires the hypothesis of a new carrier transport mechanism allowing for the characteristics of the excitation, recombination, and scattering in a pyroelectric crystal.

One such mechanism, which allows for the asymmetry of the distribution function of nonequilibrium carriers associated with the asymmetry of impurity centers, gives results which are in satisfactory agreement with experiment. The question as to what extent this mechanism describes the intrinsic (due to fundamental absorption) and not the impurity photovoltaic current has not yet been resolved. In fact, experi-

mental investigations of the intrinsic photovoltaic current have not yet resulted in reliable separation from the impurity current and should be continued (in particular, under two-photon absorption conditions). The behavior of the photovoltaic current near the ferroelectric phase transition has hardly been investigated. In the case of such crystals as KFP, whose paraelectric phase has no center of symmetry, measurements of the photovoltaic current on both sides of the Curie point should make it possible to estimate this effect in the nonpyroelectric phase without a center of symmetry. The AP effect in piezoelectric materials is still to be investigated.

There is little doubt that studies of the AP effect, which is of intrinsic interest, will make an important contribution to the physics of ferroelectricity. Moreover, this contribution should increase as the theory of the AP effect is developed.

The authors are grateful to A. P. Levanyuk for valuable discussions and many helpful comments on the manuscript.

- ¹S. M. Ryvkin, *Photoelectric Effects in Semiconductors*, Fizmatgiz, Moscow, 1963. Engl. Transl. Consultants Bureau, New York, 1973.
- ²É. I. Adirovich, In *Fotoelektricheskie yavleniya v poluprovodnikakh i optoelektronika* (in: *Photoelectric Effects in Semiconductors and Optoelectronics*), Fan, Tashkent, 1972.
- ³V. M. Fridkin, A. A. Grekov, P. V. Ionov, A. I. Rodin, E. A. Savchenko, and K. A. Mikhailina, *Ferroelectrics* 8, 433 (1974).
- ⁴A. M. Glass, D. von der Linde, D. H. Auston, and T. J. Negran, *J. Electron. Mater.* 4, 915 (1975).
- ⁵A. P. Levanyuk and V. V. Osipov, *Izv. Akad. Nauk SSSR Ser. Fiz.* 41, 752 (1977).
- ⁶V. M. Fridkin, *Segnetoélektriki-poluprovodniki* (Ferroelectric Semiconductors), Fizmatgiz, M., 1976.
- ⁷P. V. Ionov, K. A. Verkhovskaya, L. I. Ivleva, Yu. S. Kuz'minov, and V. M. Fridkin, *Kratk. Soobshch. Fiz. (FIAN SSSR)* No. 10, 24 (1973).
- ⁸P. V. Ionov, *Fiz. Tverd. Tela (Leningrad)* 15, 2827 (1973) [*Sov. Phys. Solid State* 15, 1888 (1974)].
- ⁹A. M. Glass and D. von der Linde, *Ferroelectrics* 10, 163 (1976).
- ¹⁰P. Günter and F. Micheron, Paper presented at Third Symposium on Semiconducting Ferroelectrics, Rostov-on-Don, 1976, in: *Ferroelectrics* 18, 27 (1978).
- ¹¹F. Micheron, Paper presented at Third Symposium on Semiconducting Ferroelectrics, Rostov-on-Don, 1976, in: *Ferroelectrics* 18, 153 (1978).
- ¹²I. B. Barkan, S. I. Marennikov, E. V. Pestryakov, and M. V. Éntin, *Izv. Akad. Nauk SSSR Ser. Fiz.* 41, 748 (1977).
- ¹³A. M. Glass, D. von der Linde, and T. J. Negran, *Appl. Lett.* 25, 233 (1974).
- ¹⁴V. M. Fridkin, B. N. Popov, and P. V. Ionov, Paper presented at Third Symposium on Semiconducting Ferroelectrics, Rostov-on-Don, 1976, in: *Ferroelectrics* 18, 165 (1978).
- ¹⁵V. M. Fridkin, B. N. Popov, and P. V. Ionov, *Izv. Akad. Nauk SSSR Ser. Fiz.* 42, 771 (1977).
- ¹⁶B. N. Popov and V. M. Fridkin, *Fiz. Tverd. Tela (Leningrad)* 20, 710 (1978) [*Sov. Phys. Solid State* 20, 413 (1978)].
- ¹⁷F. S. Chen, *J. Appl. Phys.* 40, 3389 (1969).
- ¹⁸K. Ohi, Y. Takeda, and Y. Ohata, *Izv. Akad. Nauk SSSR Ser. Fiz.* 41, 804 (1977).
- ¹⁹Y. Ohmori, M. Yamaguchi, K. Yoshino, and Y. Inuishi, *Jpn. J. Appl. Phys.* 15, 2263 (1976).

- ²⁰E. Krätzig and H. Kurz, *Ferroelectrics* **13**, 295 (1976).
- ²¹W. Keune, S. K. Date, U. Gonser, and H. Bunzel, *Ferroelectrics* **13**, 443 (1976).
- ²²B. Dischler and A. Räufer, *Solid State Commun.* **17**, 953 (1975).
- ²³H. Tsuya, *Izv. Akad. Nauk SSSR Ser. Fiz.* **41**, 740 (1977).
- ²⁴W. T. H. Koch, Thesis, University of Karlsruhe, 1975.
- ²⁵W. T. H. Koch, R. Munser, W. Ruppel, and P. Würfel, *Ferroelectrics* **13**, 305 (1976).
- ²⁶V. M. Fridkin, B. N. Popov, and K. A. Verkhovskaya, *Appl. Phys.* **16**, 313 (1978).
- ²⁷W. J. Merz, *Helv. Phys. Acta* **31**, 625 (1958).
- ²⁸S. G. Ellis, F. Herman, E. E. Loebner, W. J. Merz, C. W. Struck, and J. G. White, *Phys. Rev.* **109**, 1860 (1958).
- ²⁹P. S. Brody, *Solid State Commun.* **12**, 773 (1973).
- ³⁰A. A. Grekov, M. A. Malitskaya, V. D. Spitsyna, and V. M. Friedkin, *Kristallografiya* **15**, 500 (1970) [*Sov. Phys. Crystallogr.* **15**, 423 (1970)].
- ³¹T. R. Volk, A. A. Grekov, N. A. Kosonogov, and V. M. Fridkin, *Fiz. Tverd. Tela (Leningrad)* **14**, 3214 (1972) [*Sov. Phys. Solid State* **14**, 2740 (1973)].
- ³²V. M. Fridkin, V. N. Popov, and K. A. Verkhovskaya, *Phys. Status Solidi A* **39**, 193 (1977).
- ³³V. M. Fridkin, K. A. Verkhovskaya, and B. N. Popov, *Fiz. Tekh. Poluprovodn.* **11**, 135 (1977) [*Sov. Phys. Semicond.* **11**, 76 (1977)].
- ³⁴K. A. Verkhovskaya, A. N. Lobachev, B. N. Popov, V. I. Popolitov, V. F. Peskin, and V. M. Fridkin, *Pis'ma Zh. Eksp. Teor. Fiz.* **23**, 522 (1976) [*JETP Lett.* **33**, 476 (1976)].
- ³⁵G. Chanussot, V. M. Fridkin, G. Godefroy, and B. Jannot, *Appl. Phys. Lett.* **31**, 3 (1977).
- ³⁶P. Günter, U. Flückiger, J. P. Huignard, and F. Micheron, *Ferroelectrics* **13**, 297 (1976).
- ³⁷I. P. Kaminow and E. H. Turner, *Proc. IEEE* **54**, 1374 (1966).
- ³⁸P. Günter, *Opt. Commun.* **11**, 285 (1974).
- ³⁹E. Wiesendanger, *Ferroelectrics* **6**, 263 (1974).
- ⁴⁰L. A. Ivanova, V. I. Popolitov, S. Yu. Stefanovich, A. N. Lobachev, and Yu. N. Venevtsev, *Kristallografiya* **19**, 573 (1974) [*Sov. Phys. Crystallogr.* **19**, 356 (1974)].
- ⁴¹V. I. Belinicher, V. K. Malinovskii, and B. I. Sturman, *Zh. Eksp. Teor. Fiz.* **73**, 692 (1977) [*Sov. Phys. JETP* **46**, 362 (1977)].
- ⁴²V. I. Belinicher, I. F. Kanaev, V. K. Malinovskii, and B. I. Sturman, *Avtometriya* No. 4, 23 (1976).
- ⁴³É. V. Bursian, *Nelineyniy kristall: Titanat bariya (Non-linear Crystal: Barium Titanate)*, Fizmatgiz, M., 1974.
- ⁴⁴W. Jösch, R. Munser, W. Ruppel, and P. Würfel, Paper presented at Fourth Intern. Meeting on Ferroelectricity, Leningrad, 1977, in: *Ferroelectrics* (in press).
- ⁴⁵G. Chanussot and A. M. Glass, *Ferroelectrics* **17**, 381 (1977).
- ⁴⁶E. M. Baskin, M. D. Blokh, M. V. Entin, and L. I. Magarill, *Phys. Status Solidi B* **83**, K97 (1977).
- ⁴⁷V. M. Fridkin, *Appl. Phys.* **13**, 357 (1977).
- ⁴⁸A. M. Glass and D. H. Auston, *Ferroelectrics* **7**, 187 (1974).
- ⁴⁹G. A. Alphonse, R. C. Alig, D. L. Staebler, and W. Phillips, *RCA Rev.* **36**, 213 (1975).
- ⁵⁰V. I. Belinicher, *Zh. Eksp. Teor. Fiz.* **75**, 641 (1978) [*Sov. Phys. JETP* **48**, 322 (1978)].
- ⁵¹V. M. Asnin, A. A. Bakun, A. M. Danishevskii, E. L. Ivchenko, G. E. Pikus, and A. A. Rogachev, *Pis'ma Zh. Eksp. Teor. Fiz.* **28**, 80 (1978) [*JETP Lett.* **28**, 74 (1978)].

Translated by A. Tybulewicz